Supplemental Methods

Next generation sequencing. Briefly, target enrichment was performed with 2 µg genomic DNA using the SureSelectXT Human All Exon Kit version 6 (Agilent) to generate barcoded whole-exome sequencing libraries. Libraries were sequenced on the HiSeqX platform (Illumina) with 50x coverage. Quality assessment of the sequence reads was performed by generating QC statistics with FastQC. The bioinformatics filtering strategy included screening for only exonic and donor/acceptor splicing variants. In accordance with the pedigree and phenotype, priority was given to rare variants (<0.01% in public databases, including 1000 Genomes Project, NHLBI Exome Variant Server, Complete Genomics 69, and Exome Aggregation Consortium [ExAC v0.2]) that were fitting a recessive (homozygous or compound heterozygous) or a *de novo* model and/or variants in genes previously linked to neuropathy, developmental delay, and other neurological disorders. Haplotype analysis was done by plotting a colour banding of the variants flanking the pathogenic ARHGAP19 variants for affected individuals and control samples. By comparing the banding patterns of patients and controls, the status of being a founder/recurrent variant was investigated. In the case of founder variants, we estimated the age of the most recent common ancestor (MRCA) using the length of shared haplotypes between patients.

Calculation of free energy changes. The AlphaFold2 derived wild-type ARHGAP19 protein structure was energy minimised and prepared for mutagenesis with the 'RepairPDB' and 'BuildModel' commands in FoldX, respectively. Subsequent free energy calculations were performed with the 'Stability' command, and differences in free energy were determined by subtracting the free energy value of the wild-type protein monomer from that of the mutant protein ($\Delta G_{MUT} - \Delta G_{WT}$). Calculations were replicated 10 times with default parameters for each substitution. Substitutions were classified as having a destabilising effect on protein folding if the free energy difference ($\Delta\Delta G$) was >1.6 kcal/mol.

Cell culture of primary dermal fibroblasts

Primary dermal fibroblasts were obtained from family 5 (P5 (F5-II:2) (c.419G>A), family 6 (P6 (F6-II:7) (c.203T>C) and family 10 (P11 (F10-II:1) (c.85A>G) and age/ gender matched control individuals. Fibroblasts were cultured in Dulbecco's modified Eagle medium (Thermo Fisher Scientific) supplemented with 10% fetal bovine serum (GE Healthcare) and penicillin-streptomycin (100 U/mL and 100 mg/mL, respectively; Thermo Fisher Scientific).

Differentiation of iPSCs to spinal motor neurons. Briefly, iPSCs were dissociated with accutase and resuspended in a 10mm2 Petri dish to form embryoid bodies (EBs). Differentiation medium consisted of (1:1 DMEM/F12-Neurobasal media, supplemented with N2, B27, 2 mM L-glutamine, 1% Pen-Strep, 0.1 mM β-ME; all from ThermoFisher Scientific), with 10 μM Y-27632 (Tocris), 0.1 μM LDN 193189, 20 μM SB431542, and 3 μM CHIR-99021 (Cambridge Bioscience). Media was replaced every 2-3 days, with the addition of the following small molecules: 100 nM retinoic acid (RA, Sigma Aldrich) from day 2; 500 nM Smoothened Agonist (SAG, Sigma Aldrich) from day 4; 10 μM DAPT (Cambridge Bioscience) from day 9. LDN 193189, SB431542 and CHIR-99201 were discontinued on day 7. The neurotrophic factors BDNF, CNTF and GDNF (Peprotech) were added to the differentiation medium from day 11, at a concentration of 10 ng/mL. On day 14, EBs were dissociated, and post-mitotic neurons were seeded on poly-L-ornithine (Sigma Aldrich) and laminin (Biotechne) coated plates.

RT-qPCR from patient-derived fibroblasts

Total RNA was extracted from cultured primary fibroblasts of subjects P5 (F5-II:2), P6 (F6-II:7), and P11 (F10-II:1) and controls and from iPSC motor neuron of subjects P5 (F5-II:2) and P6 (F6-II:7) and controls (QIAGEN RNeasy). gDNA purification was performed with DNA-*free*™ DNase (Thermofisher). 0.5 μg total RNA was reverse transcribed (Superscript III, Thermofisher). Technical triplicates of RT-qPCR samples were prepared with Fast SYBR™ Green Master Mix (Thermofisher).

Western blotting

Fibroblasts of subjects P5 (F5-II:2), P6 (F6-II:7) and P11 (F10-II:1) and controls and fibroblast-derived iPSc motor neurons of patients subjects P5 (F5-II:2) and P6 (F6-II:7) and controls were lysed in ice-cold RIPA buffer supplemented with Mini Protease Inhibitor (Roche). Protein extracts were loaded on 4-12 % SDS polyacrylamide gel, transferred to polyvinylidene fluoride membranes and blocked and incubated overnight with ARHGAP19 primary antibody (Santa Cruz Biotechnology; 1:500). Secondary antibody HRP-linked anti-mouse (#G-21040 Invitrogen; 1:10,000) was added for 1 h. Immunoblots were digitally imaged with iBright 750 (invitrogen) and band intensities were determined using Image Lab v6.0 software (Bio-Rad). GAPDH (ab9484, Abcam; 1:10000) was used as a loading control. Blots were repeated in duplicates, statistics were performed using GraphPad Prism and the significance between variables was shown based on the p-value obtained (ns indicates $p > 0.05$, *$p < 0.05$, **$p < 0.005$, ***$p < 0.0005$, ****$p < 0.00005$).

iPSC motor neuron immunofluorescence. Post-mitotic neurons were seeded on poly-L-ornithine (Sigma Aldrich) and laminin (Biotechne) coated plates at 15,000 cells per well and fixed at day 18 with 4% PFA for 20 mins. After permeabilization with 0.2% Triton-X-solution for 30 mins at room temperature, the cells were blocked with goat serum (5% in PBT), and incubated with anti-beta-3-tubulin mouse monoclonal antibody (2434344, Invitrogen; 1:500 dilution) overnight at 4°C.
After four washing steps (PBT), the cells were incubated with Alexa Fluor™ anti-mouse 488 secondary antibody (A11001, ThermoFisher; 1:1000 dilution) in the dark at room temperature. For nucleus detection, the cells were incubated with DAPI (D1306, ThermoFisher; 1:1000) under dark conditions and high-resolution images were acquired using Leica Mica confocal microscope at 20x magnification to assess motor neuron morphology.

Sholl analysis. Neurite complexity of iPSC derived motor neurons of patients P5 (F5-II:2) and P6 (F6-II:7) and controls ($n = 5–10$ cells per group) was analysed by Sholl analysis. Maximum intensity projections of z-stacks and only morphologically isolated neurons were used for the analysis. Images were processed using ImageJ (Version 1.54p), Neuroanatomy, Sholl analysis plugin. Sholl analysis was performed with concentric circles spaced at 5µm intervals radiating

outward from the soma. For each neuron, the number of intersections at each radius was calculated and maximum number of intersections and distance from soma (in μm) were used as summary metrics for branching. Comparisons between the neurite branching and neurite lengths in the groups were conducted using the Kruskal–Wallis test.

Migration assay. 100,000 cells were resuspended in serum-free medium and plated on the top chamber (24-well transwell insert, Falcon: 353097). Cells were incubated at 37°C for 24h, which

then washed five times with PBS followed by one wash with water before mounting onto coverslips with Prolong Diamond Antifade Mountant (Invitrogen). Images were acquired on a Zeiss LSM510 confocal laser-scanning microscope equipped with a Plan Neofluar 40x/1.30 oil DIC microscope objective and the Zen 2009 software (Carl Zeiss). Quantification of the aspect ratio (length/width) was calculated with ImageJ software.

RT-qPCR from patient derived fibroblasts. RT-qPCR samples were prepared in 10µl reactions with Fast SYBR™ Green Master Mix (Thermofisher) with 500 nM of each primer, and 1 µl of the reverse transcription reaction. Primer sequences for RT-qPCR are described in Supplemental Table 6**.** RT-qPCR was performed using the QuantStudio 3 Real-Time PCR System (Thermo Fisher Scientific). The PCR conditions included a pre-run at 95°C for 5 min, followed by 40 cycles of 30 s at 95°C, 30 s at 58°C and 45 s at 72°C. PCR amplification specificity was determined by melting curve analysis with a range from 60°C to 95°C. The values of the cycle threshold (∆CT) of the target mRNAs were normalized to the mRNA of *RPL18* using QuantStudio Design&Analysis Software (Thermo Fisher Scientific) and expressed as x-fold change to controls.

RNAseq analysis. Pools were sequenced using the Illumina NovaSeq 6000 Sequencing system to generate 100 bp paired-end reads with an average read depth of ~100 million reads per sample. RNA sequencing raw data was mapped to human reference genome assembly hg38 using STAR (44). Gene count tables were imported into R environment to analyse differential gene expression patterns using DESeq2 package (45). For gene enrichment analysis, pathfindR package was employed (46). Briefly, Biogrid database was used for mapping the genes to protein-protein interaction network, with their associated p-values. The resulting active subnetworks were filtered based on the significant genes they contain. The filtered subnetworks were then enriched by the related cellular pathways. This was followed by hierarchical clustering to group biologically relevant pathways. Major pathways with enrichment fold greater than 2 were selected for plotting per sample expression scores.

Zebrafish. Genomic deletions were introduced at three selected loci within the zebrafish arhgap19 gene—exons 2, 4, and 5—informed by considerations of targeting efficiency and potential off-target effects. Nine crRNAs were designed according to their on-target and off-target scores. The six sgRNAs sequences were: 1) 5'-ACGCTCCTCAAGAGTTTCTT-3', 2) 5'-CAAGATGTCTGCTCACAACC-3', 3) 5'- CAAGAGTTTCTTGGGAGAAT-3', 4) 5'-GAACCCAAGACTCCCAACGC-3', 5) 5'-TGACTTTCATCCCAATGACG-3', 6) 5'-AGGCAACAAGACGAGTTTTC-3', 7) 5'-CCGGCTCATCGACCTCCCAG-3', 8) 5'-GAGTTCCTGGGAACAGTCTG-3', and 9) 5'-AGGAGTGTTCGGTTGGCGGT-3'. Each cRNA was annealed to tracrRNA and complexed to Alt-R S.p. HiFi Cas9 nuclease to form a ribonucleoprotein (RNP). A pool of three RNPs were co-injected into one cell stage zebrafish embryos. Of the initial batch of 62 eggs, 32 (51.6%) were successfully fertilized. Embryos were monitored on a daily basis, with dead ones discarded. Those that survived were sacrificed at 5 dpf for genotyping and subsequent analysis. Three zebrafish larvae were randomly selected for genomic DNA extraction to determine the targeting efficiency. PCR amplification targeting RNP cut sites were performed for each crRNA and products purified, pooled and sent for next generation sequencing. Primers included universal adaptors for Illumina MiSeq (Eurofins). Cut efficiency was calculated for each RNP using CRISPResso2 and High-Resolution Melting curve analysis.

***Drosophila* Off-target analysis.** To reduce off-target effects, CRISPR/Cas9 guides were selected using the CRISPR Optimal Target Finder Tool (http://targetfinder.flycrispr.neuro.brown.edu). Guides that are predicted to only cut at the RhoGAP54D locus were selected. Additionally, upon generation of the *RhoGAP54D*^{KO} allele, the potential off-target mutations are eliminated by out-crossing the parental chromosomes to remove the vas-Cas9 insertion.

***Drosophila* activity assays.** Individual flies were housed in glass tubes containing 4% sucrose and 2% agar, bisected by an infrared beam, allowing activity to be quantified as the number of beam breaks made by each fly over time. Fly movement was measured at 25°C across 24 h comprised of 12 h light and 12 h dark period, from which total activity and activity during ZT

(zeitgeber time) 12-13 were quantified. Experiments were performed on 3-7 day old male flies. All flies were acclimatised to the DAM conditions for 48 h prior to the experimental period.

***Drosophila* IHC.** Briefly, brains were fixed for 20 min at room temperature via incubation in 4% paraformaldehyde (MP Biomedicals), and blocked for 1 h in 5% normal goat serum in Phosphate Buffered Saline containing 0.3% Triton-X (Sigma-Aldrich) (0.3% PBT).

Larval crawling assay. Video-based recordings of *RhoGAP54D*^{KO} heterozygote and homozygote 3rd instar larvae were performed over 30 s on an agar surface, following an initial 1 min of acclimatisation at room temperature. Traces of peristaltic locomotion were measured using a Raspberry Pi Virtual Reality System (PiVR)(50). Mean distances travelled over 30 s in *RhoGAP54D*^{KO} heterozygote and homozygote larvae were quantified via PiVR.

RhoGap NMJ imaging analysis. Wandering 3rd instar "wandering" larvae were dissected in ice-cold phosphate-buffered saline (PBS) (Sigma Aldrich), fixed for 25 mins at room temperature in 4% paraformaldehyde (MP biomedicals), blocked for one hour in 5% goat serum in PBS + 0.3% Triton-X (Sigma-Aldrich) (PBT), and incubated overnight in Alexa Fluor® 488 AffiniPure™ Goat Anti-Horseradish Peroxidase (Jackson Immunoresearch), which labels *Drosophila* neuronal membranes. Images were taken with a Zeiss LSM 710 confocal microscope with an EC 'Plan-Neofluar' 40x/0.50 M27 oil immersion objective, taking z-stacks through the NMJ with step sizes of 1-2 µm. Image analysis was performed using Fiji (ImageJ). Z-stacks of the whole brain were projected using a maximum intensity projection. Boutons were manually counted. Projection length was calculated by drawing freehand lines along each projection and summing total length. Bouton surface area was calculated by drawing freehand lines around 10 boutons per NMJ, excluding the last bouton on each projection, and taking a mean of the areas.

Zebrafish Off-target Analysis. Potential off-target sites caused by sgRNA were predicted using IDT design checker. Top two predicted off-target genes for each crRNA were selected for

analyzing the off-target effects. Off-target genes were amplified by PCR, follow by Sanger Sequencing. The primers for amplifying the possible off-target genes are shown below.

crRNA	Primer	Sequence (5'–3')
AD	Off-target gene 1 CCNI2 forward	ACTAGGGCTGCACGGATAAA
	Off-target gene 1 CCNI2 reverse	GAATTCTTTCAAAGGCCTCCAA
	Off-target gene 2 TRIM46A forward	TGTGTGCAGTCTAACATGAAGAG
	Off-target gene 2 TRIM46A reverse	TCACAAATCAGATGAACAGAGGT
AK	Off-target gene 1 ALOX5B.3 forward	ACTAGAGAGAGGGAGATGGTGT
	Off-target gene 1 ALOX5B.3 reverse	GGCTAACAACCAGTCGTAGTG
	Off-target gene 2 PROSC forward	GCGAGAGTCTGAAGATCCCA
	Off-target gene 2 PROSC reverse	CCACAAGTATTTTACACAGGGCT
AH	Off-target gene 1 FRAS1 forward	AAACGAGAACAAACCCACTCT
	Off-target gene 1 FRAS1 reverse	AGCTGGTGCATAAAGAAGGCT
	Off-target gene 2 SLC5A8 forward	TCTCTTTCAGCTTCGACCCA
	Off-target gene 2 SLC5A8 reverse	CTGCCACAAACAACCCTGG

RNA sequencing from Zebrafish tissue, bioinformatic analysis, and statistics

Contaminating adapter sequences and low-quality base were trimmed from the FASTQ files using fastp (56). FASTQ files were aligned to the Danio_rerio.GRCz11.dna.primary_assembly reference genome using STAR aligner (version 2.7.11b). Read counting of protein coding exons (Danio_rerio.GRCz11.96.gtf as reference) was performed by "summarizeOverlaps" function in GenomicAlignments (version 1.8.4) implemented in R version 4.3.2. Differential expression of Ensembl annotated genes was determined using the DEseq2 package in R with padj <0.05 considered to be significant. Principle Components (PC's) were also calculated using DESeq2. Volcano plots were also created using custom R scripts and ggplot2. Spearman's correlation

coefficient was calculated using the R base package and then visualised on a heatpmap using the pheatmap package.

Additional Acknowledgements. JP is supported by Medical Research Future Fund (MRFF) Genomics Health Futures Mission (APP2007681) and by the Australian Government Research Training Program. LVdV is supported by a predoctoral fellowship of the Research Fund - Flanders (FWO) under grant agreement N°11F0921N. TS is member of the European Reference Network for Rare Neuromuscular Diseases (ERN EURO-NMD). JB is supported by a Senior Clinical Researcher mandate of the Research Fund - Flanders (FWO) under grant agreement N°1805021N. ANB gratefully acknowledges the support of SVIKV and the use of the services and facilities of the Koç University Research Center for Translational Medicine (KUTTAM), funded by the Presidency of Turkey, Head of Strategy and Budget. We thank collaborator Simon Bullock (University of Cambridge) for plasmids, and Florencia di Pietro for characterization of the RhoGAP54D LOF allele. JECJ is funded by an MRC Senior Non-Clinical Fellowship (MR/V03118X/1), SL by a BBSRC Project Grant (BB/X00094X/1), and AW by a Wellcome Early Career Award (308298/Z/23/Z). Work in the Bellaïche group is funded by the CNRS, the INSERM and the Institut Curie as well as by the ANR (TiMecaDiv 20CE13000801) grant. TBH was supported by the Deutsche Forschungsgemeinschaft (DFG, German Research Foundation – 418081722, 433158657), and the European Commission (Recon4IMD - GAP-101080997). This work was supported in part by the Fund for Scientific Research (FWO-Flanders) (research grants G048220N and G0A2122N to A.J.), the Research Fund of the University of Antwerp (doctoral grant to C.A.), the Association Belge contre les Maladies Neuromusculaires' (ABMM-Telethon) (research grantsto A.J.), the French Muscular Dystrophy Association (AFM-Telethon, research grant 23708 to A.J.). JPark was supported by the Clinician Scientist program "PRECISE.net" funded by the Else Kröner-Fresenius-Stiftung. Work in the Lamarche-Vane group funded by Natural Sciences and Engineering Research Council of Canada grant RGPIN/04809-2017 and CIHR project grant PJT-180367. LL holds a CIHR master studentship. RH is supported by the Wellcome Discovery Award (226653/Z/22/Z), the Medical Research Council (UK) (MR/V009346/1), the Addenbrookes Charitable Trust (G100142), the Evelyn Trust, the Stoneygate Trust, the Lily Foundation, Ataxia

UK, Action for AT, the Muscular Dystrophy UK. MCFJ is supported by Fundação de Amparo à Pesquisa do Estado de São Paulo (FAPESP) grant # 2021/06739-4. This research was supported by the NIHR Cambridge Biomedical Research Centre (BRC-1215-20014). The views expressed are those of the authors and not necessarily those of the NIHR or the Department of Health and Social Care. ANB gratefully acknowledges the support of SVIKV and the use of the services and facilities of the Koç University Research Center for Translational Medicine (KUTTAM), funded by the Presidency of Turkey, Head of Strategy and Budget. Muge Kovancılar Koç and Irmak Şahbaz are greatly acknowledged for their excellent technical assistance. We are also grateful to Queen Square Genomics at the Institute of Neurology University College London, supported by the National Institute for Health Research University College London Hospitals Biomedical Research Centre, for the bioinformatics support. MMR is grateful to the Wellcome Trust (G104817), National Institutes of Neurological Diseases and Stroke and office of Rare Diseases (U54NS065712 and 1UOINS109403-01), Muscular Dystrophy Association (MDA510281), Charcot Marie Tooth Association (CMTA), Harrington Discovery Institute, Alnylam Pharmaceuticals and Applied Therapeutics for their support. This research was also supported by the National Institute for Health Research University College London Hospitals Biomedical Research Centre. The zebrafish model was supported by Sidra Medicine, Research Branch, Zebrafish Facility R & D Budget. We thank Mr. Waseem Hasan and Ms. Doua Abdelrahman for their technical support in zebrafish experiments.

Online resources

CPDB web tool, http://cpdb.molgen.mpg.de/

Ensembl, http://www.ensembl.org/i

FastQC, http://www.bioinformatics.babraham.ac.uk/projects/fastqc/

GATK documentation, https://software.broadinstitute.org/gatk/

GTEx, https://www.gtexportal.org/home/

Human Genome Variation Society, http://www.hgvs.org

IDT design checker, https://eu.idtdna.com/site/order/designtool/index/CRISPR_CUSTOM

Mutation Taster version 2, http://www.mutationtaster.org/

PolyPhen-2, http://genetics.bwh.harvard.edu/pph2/

SIFT, http://sift.jcvi.org/

University of California—San Francisco (UCSC) Genome Browser, https://genome.ucsc.edu/

Jalview, https://www.jalview.org/

UniProt, https://www.uniprot.org/

PyMol, https://pymol.org/2/

AlphaFold Protein Structure Database, https://alphafold.ebi.ac.uk/

FoldX, https://foldxsuite.crg.eu/

DIOPT http://flybase.org/reports/FBgn0034249.html

Clinical Vignettes

Family 1 P1 (F1-II:1)

A previously healthy male patient from consanguineous parents aged 6 years developed distal atrophy of the lower limbs, progressive falls, and progressive worsening of gait. He presented to our clinic aged 8. On examination he had asymmetric weakness of distal lower limbs left more than right, with normal sensory and upper limb examinations. Neurophysiology of lower limb motor nerves only revealed a length-dependent neuropathy.

Family 2 P2 (F2-II:5)

The patient (now 21 years old) was born of non-consanguineous parents. He developed progressive difficulty in walking starting aged 7 years. He complained of flat feet which developed with progression of his condition due to wasting of small muscles of the foot. He reported that his right LL was more affected than the left LL. He developed marked weakness of the toes and ankle with foot drop on the left side. There is a history of numbness of both feet. There is no history of pelvic girdle muscle weakness. He noticed progressive hypertrophy of calves bilaterally. There is no history upper limb weakness. The patient walks without support. Neurological examination showed normal upper limbs, flat feet and hammer toes, hypertrophy of calves bilaterally (Pseudohypertrophy),

weakness: toes and ankles: left: grade 1, right 1-2, normal power knees and hips, brisk knee and ankle deep tendon jerks, normal abdominal reflexes, stocking hypesthesia, flexor plantar responses. Investigations: Axonal and demyelinating neuropathy (mainly axonal) in both lower limbs, more on the left side.

Family 3 P3 (F3-II:1)

16-year-old female from consanguineous parents was assessed. Her presentation was of falls starting aged 9 years. Examination showed bilateral asymmetric foot drop L>R, with distal lower limbs wasting and asymmetric weakness. The patient was areflexic and there were no sensory signs or symptoms. Neurophysiology showed a pure motor neuropathy with clear conduction slowing in the intermediate range with partial conduction block in left ulnar and possible block in posterior tibial nerves.

Family 4 P4 (F4-II:1)

A female presented with distal weakness of the lower limbs, onset at 10 years. On examination there was length dependent muscle atrophy and weakness, with sensory abnormalities and bilateral *pes cavus*. Serial NCS showed a slowly progressive length-dependent motor > sensory axonal neuropathy. Additional nerve ultrasound studies of bilateral median ulnar, peroneal, tibial , sural and sciatic nerves, and left and right brachial plexus (2020) showed a gracile aspect of these nerves, all with normal cross-sectional areas. No additional demyelinating features were found. In 2014, a muscle CT with selected transversal views of the cervical, thoracal and abdominal muscles and muscles of the upper and lower extremities, was performed, showing minimal atrophy and fatty infiltration of the upper leg, moderate atrophy and fatty infiltration of the lower leg (Goutallier grade 1-2) and severe atrophy with fatty infiltration of the feet (Goutallier grade 3).

Family 5 P5 (F5-II:2)

A male in his forties presented in his teens with progressive difficulty in walking with progressive distal weakness of both lower limbs. On examination there was wasting of both anterior and posterior leg muscles and feet. Power was normal in the upper limbs. Distal predominant weakness was seen in the lower limbs (Knee flexion grade 4, knee extension asymmetric grade 4, ankle flexo-extension 0). All lower limb reflexes were absent except for a reduced right patellar jerk. There was no sensory involvement. Neurophysiology showed motor-predominant LL predominant axonal neuropathy. Leg MRI showed complete muscle atrophy in feet in all compartments in calves with cattered patchy fatty infiltration on thigh muscles.

Family 6 P6 (F6-II:7)

A female 17-year-old from consanguineous parents was assessed. Symptom onset was in the first year of life with difficulty walking and falls. Initially there was predominance of the right lower limb. At 12 years there was a 4-month progression of left lower limb weakness. There are no sensory symptoms. She was currently being treated with regular subcutaneous immunoglobulin. On examination there was wasting of intrinsic foot muscles, thickening of skin on palms and soles of feet, and an asymmetric steppage gait. She had difficulty walking on toes R>L and could not stand on heels. There was no clear proximal weakness and tandem walk was normal. There was distal lower limb weakness right worse than left. Reflexes were preserved at the knee, absent at the ankle. There were abnormalities to vibration distally. Neurophysiology showed a lower limb predominant motor neuropathy with conduction slowing in lower limbs. CSF studies had previously shown a high protein.

Family 7 P7 (F7-II:1)

A 13-year-old female had distal weakness of the legs aged 11. She has symptoms of glove and stocking hypoaesthesia. On examination there was mild bilateral *pes cavus* with atrophy of the small muscles of the feet and high stepping gait. There was distal

weakness of lower limbs. Muscle power of distal lower limbs was grade 4. She was areflexic in lower limbs. Neurophysiology showed mixed axonal and demyelinating neuropathy (mainly axonal) in both upper and lower limbs and neurogenic lower limb EMG.

Family 8 P8 (F8-II:2)

A 48-year-old female patient whose disease started at the age of 11 with walking difficulties. She used to trip and fall easily. The disease progressed slowly. Her parents were first degree relatives. On examination there was severe weakness in peroneal innervated muscles. Sensation was decreased in a length dependent pattern. EMG suggested a motor predominant axonal neuropathy with a striking asymmetry left much more severe than right in upper limbs.

Family 9 P9 (F9-II:3) and P10 (F9-II:4)

P9 (F9-II:3), a 20-year-old patient is the first-born child of healthy consanguineous parents of Syrian origin. His child development stages were normal; he did not have any motor or language developmental delay. He first noticed gait difficulties due to right foot drop at the age of 15 years old. A few months after the onset of initial symptoms, the left foot showed weakness as well. On examination, he presented with a high stepping gait, weak dorsiflexion of both feet and all toes, stocking hypoesthesia and diminished deep tendon reflexes with clinically intact proprioception and nociception, and was diagnosed with severe sensorimotor polyneuropathy. The disease progressed slowly over the years, but other extremities were not affected. The left foot always showed a milder foot drop than the right foot. He is ambulant and is able to walk and run with leg braces. . Otherwise, other medical complications or skeletal deformities were not reported. He had slightly elevated CK levels (220 – 350 U/l) and a slightly elevated CSF protein (477mg/L). He has three younger sisters, and the youngest sister (patient 2) is similarly affected. Other affected family members are not known. One sister of his mother has an intellectual

disability due to a childhood accident. The grandparents of his parents are siblings (pedigree).

P10 (F9-II:4)is a 13-year-old patient is the youngest sister of patient 1. She developed symmetric weakness of both feet at the age of 9 years old. On clinical examination at age 13 years, she showed severe predominantly demyelinating sensorimotor polyneuropathy. She presented symmetric, marked weakness in dorsiflexion of feet with unobtainable tendon reflexes and mild weakness of the right hand with reduced fine motor skills. Pinprick sensation was normal in the limbs, but vibration sense was severely reduced in both distal lower limbs. Electrophysiological examination revealed no response for motor and sensory nerves in the lower limbs and reduced sensory nerve conduction velocity and amplitude in the right hand. She ambulates with foot drop splints and falls frequently. Her cognition is normal.

Family 10 P11 (F10-II:1)

A 68-year-old man from consanguineous parents was first assessed in the clinic aged 59. Aged 30 he developed cramps in his legs which was his initial symptom. He had been seen in a number of specialist clinics to investigate causes of muscle hyperexcitability including autoimmune and genetic channelopathies, before it emerged neurophysiologically that this was a neuropathy. He developed slowly progressive weakness of his lower limbs with no sensory symptoms. On examination aged 59 he had a normal upper limb examination. Lower limb examination showed distal muscle atrophy, ankle dorsiflexion weakness grade 4/5 bilaterally with full proximal power. At that time his reflexes were all present. There were distal abnormalities to pinprick, vibration was absent to the hip on the right and knee on the left. With time he developed proximal weakness in the lower limbs and minor hands weakness. Neurophysiology showed a length-dependent sensory and motor neuropathy, but with some acute denervation demonstrated in previous

studies. MRI demonstrated some white matter changes consistent with small vessel ischaemia.

Family 11 P12 (F11-II:2)

The male proband was born to healthy consanguineous parents of Italian heritage. There are also two healthy siblings of the proband. There is no family history of neuromuscular disease in the family. The proband was thirteen at the onset of disease and presented progressive weakness of distal lower limbs. Clinical examination of the proband at 15 years of age revealed bilateral foot drop and high steppage gait with mild *pes cavus*. Joint position sense and pinprick response in the feet were reduced, with absent ankle reflexes. The proband was unable to dorsiflex or evert ankles and showed reduced power ankle plantarflexion and inversion. Neurophysiology showed a length dependent motor-predominant axonal neuropathy with some conduction slowing.

Family 12 P13 (F12-II:1)

An 11-month boy born from consanguineous parents presented with increasing weakness and loss of function of upper limbs over 15 days with severe pneumonia. There was reported mild weakness of lower limbs preceding this event. MRI of spine was normal, MRI of brain revealed mild hypoplastic BL temporo-parietal region. Neurophysiology at this stage was not performed. EEG was normal. He was discharged with improvement of the condition. At 3 years old he was improving functionally and started walking with the help of walker, could say simple sentences, he had regained upper limb function, his cognition seemed better compared to his motor disability. Sadly, the child died at 3 1/2 years with a sudden convulsion having lost consciousness then died within 10 minutes; acute stroke was suspected.

Family 13 P14 (F13-II:3)

No clinical information available.

Family 14 P15 (F14-II:2)

A male from consanguineous parents presented aged 11 years with frequent falls. On examination se had bilateral steppage gait and *pes cavus*. There was weakness of the intrinsic muscles of the hands, distal atrophy in the lower limb. There was no sensory loss. He was areflexic. Her neurophysiology reportedly showed a motor axonal neuropathy.

Family 15 P17 (F15-II:2)

A 13-year-old female presented with acute painless left-hand weakness after the hand was struck by a ball. Initial examination showed thinning of hand muscles L>R. She walked with mild foot drop. There was mild distal extremity weakness worst in left hand. She had distal hypoaethesia and decreased reflexes in upper and lower limbs. Neurophysiology performed 10 days after the injury suggested a left ulnar neuropathy on a background of a widespread slightly patchy sensory and motor (motor predominant) neuropathy with conduction slowing. She was treated with steroids initially. Further assessment and investigations: echocardiogram – significant mitral valve insufficiency, normal ophthalmic examination, normal hearing assessment, normal lipid profile, normal CSF profile. PMP22 copy number was normal. She was started on intravenous immunoglobulin for treatment of presumed CIDP and received multiple courses. Examination approximately two years later showed mild scoliosis, some thinning of hand muscles left >right, hammer toes. There were subtle added movements of the hands when outstretched. She had intrinsic hand muscle weakness of left more than right hand, and weakness of only extension of the great toe in the lower limb. There was mild reduction in distal temperature sensation but grossly preserved vibration sense. Reflexes were patchily reduced in upper limbs, brisk at the knees with spread, and present at the ankles. Plantars down going, she could stand on heels and toes and run, with slightly clumsy gait. Neurophysiology 18months after the initial presentation showed a length dependent motor predominant demyelinating neuropathy.

Family 16 P18 (F16-II:1)

A 15-year-old female presented with left foot drop, followed by right foot drop and numbness since the age of 12. She is still independently ambulating. Examination showed normal power in proximal upper limbs, +4/5 distal weakness in arms, normal force in proximal lower limbs, 0-1/5 distal weakness in lower limbs (Lt>Rt), distal sensory loss (pinprick, temperature, and position) in distal lower limbs, upper limbs are almost intact. Upper limbs +1 DTRs, Lower limbs Absent DTRs (areflexia)

Family 17 P19 (F17-II:1)

A 10-year-old female from consanguineous parents. The patient presents with 1.5-year history of right leg weakness (onset at 8 years). Examination showed right foot dorsiflexor weakness, decreased/absent ankle reflexes. NCS showed axonal and demyelinating changes on both legs. MRI spine: diffuse reduction in calibre of the dorsal spinal cord, syringomyelia, Normal brain MRI. Normal muscle biopsy. Normal right sural nerve biopsy.

Family 18 P20 (F18-II:1)

A 9-year-old female consanguineous parents. Presented with ascending weakness, initially asymmetrical started from right leg more than left leg within a year, upper limbs clinically spared. Examination showed severe bilateral steppage gait right more than left, with distal wasting, atrophy and weakness, without sensory involvement. NCS showed a conduction slowing motor neuropathy and MRI spine showed minor non-compressive disc bulges.

Family 19 P21 (F19-II:1)

A 16-year-old male from consanguineous parents. He was born of a normal birth and walked at 11 months. Aged 11 he started to avoid running races. Aged 13 he could not lift the left foot off the floor. There has been progressive weakness. He denies any sensory loss or pain. He has no symptoms in the upper limbs. On examination he walked with a

marked left foot drop. There was quite significant left ankle instability and pes planus. He can stand on his toes individually but not his heels. The cranial nerves were normal. There was no scapular winging or significant scoliosis. Tone and power were normal in the upper limbs. In the lower limbs he had definite weakness of ankle dorsiflexion bilaterally, grade 4 on the right, zero on the left. Plantar flexion was grade 5. Inversion 4 on the left, 5 on the right and eversion 4 on the right and 5 on the left. Reflexes were all present including at the ankles. Sensory examination was normal. He has had MRI of the brain, spinal cord and lumbar plexus which show no cause. His nerve conduction studies show denervation bilaterally in both tibialis anterior muscles. His abductor hallucis CMAPs are slightly small.

Family 20 P25 (F21-IV:I), P22 (F21-II:2), P23 (F21-II:3), P24 (F21-II:4)

IV:1: The proband is 5-year-old girl from consanguineous parents who presented with distal bilateral foot drop when she was 3 years old. The disease followed a slowly progressive course. On examination ages 3 ½ years strength in TA/EHL was MRC 2/5 , and gastrocnemius 4+/5. The remaining muscles showed normal power. Sensory examination was normal. Ankle jerks were absent and there was an asymmetry of knee/upper limb reflexes. Neurophysiology showed an axonal motor neuropathy.

II:2: The oldest paternal great-aunt is 54-year-old, and her disease began with symmetric foot deformities aged 12 years. Her disease slowly progressed, but was confined to the legs for 25 years. On examination there was mild weakness in TA but otherwise normal motor examination. She has mild distal sensory disturbance and widespread areflexia. She had an intention tremor.

II.3: The middle paternal great-aunt is 46 years old and her disease began with left foot drop aged 5 years. This remained stable for 6 years, then spread to the right leg. On examination power in TA/EHL was MRC 1/5 , and gastrocnemius 3/5, knee extension 4/5.

Upper limb motor examination was normal. She has mild distal sensory disturbance and widespread areflexia. She had an intention tremor.

II.4: The youngest paternal great-aunt 41 yo lady developed right foot drop aged 7 years. It remained stable for 5 years and then spread to the left leg. On examination power in TA/EHL was MRC 4/5 , and gastrocnemius 4+/5, the rest of the motor examination was normal. Sensory examination was normal. Lower limb reflexes were absent.

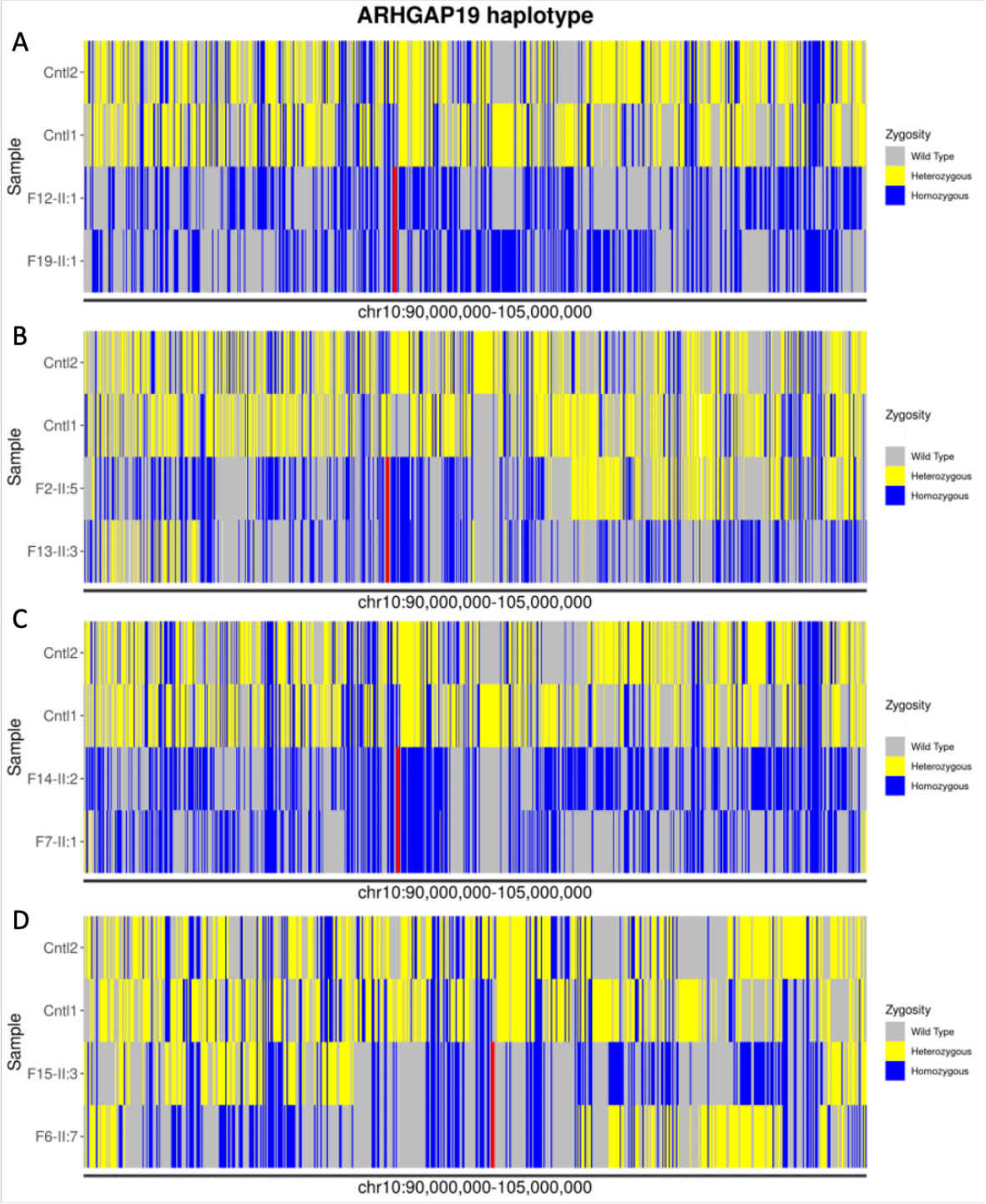

Supplemental Figure 1. Haplotype analysis of *ARHGAP19* variants A. chr10-97259559-A-T (p.Leu228His) **B.** chr10:97263447-G-GT (p.His196Gln*fs**9) **C.** chr10-97263582-G-T (p.Gln151Lys) and **D.** chr10-97265979-A-G (p.Leu68Pro). Variations pattern of flanking regions of shared pathogenic variants was coloured as follows: homozygous variants as blue, heterozygous variants as yellow, and WT locus as grey. The position of the pathogenic variant is highlighted in red.

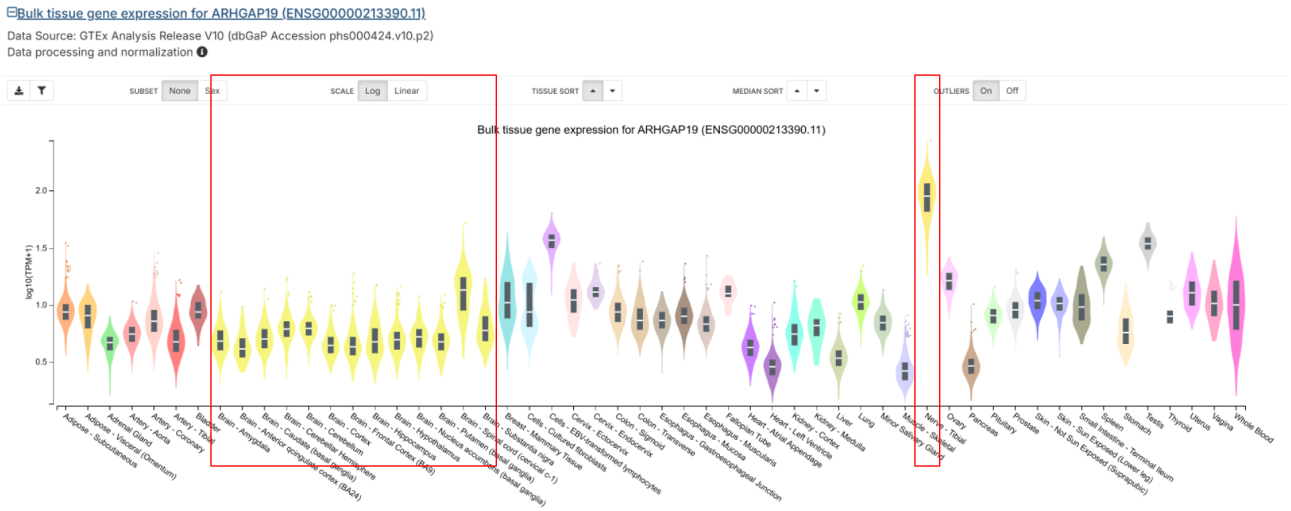

Supplemental Figure 2. ARHGAP19-Gene expression in different tissues from GTEx Portal.

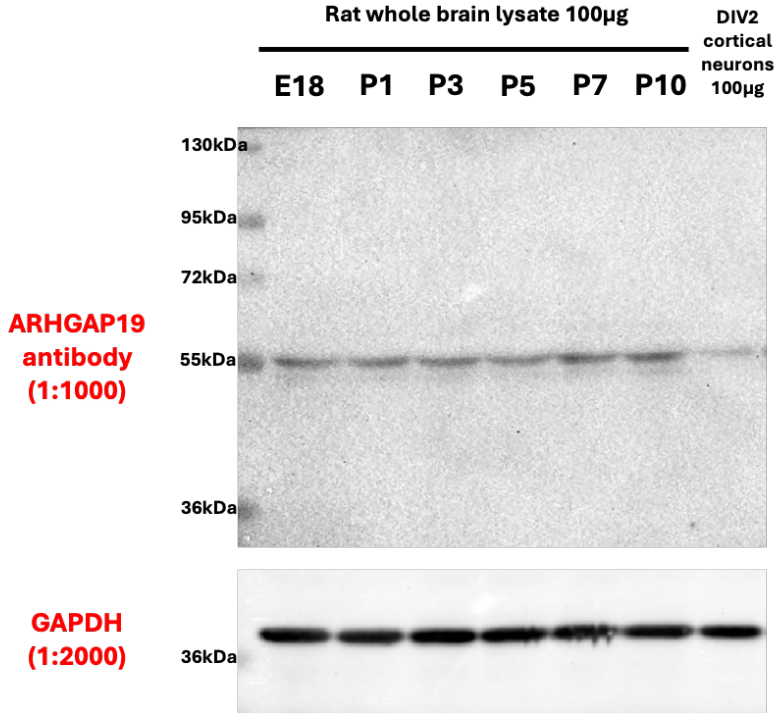

Supplemental Figure 3. Developmental expression of ARHGAP19 in rat whole brain. Homogenates of rat whole brain from embryonic day 18 (E18) till postnatal day 10 (P10), or lysates of E18 cultured cortical neurons at days in vitro 2 (DIV2) were resolved by SDS-PAGE and the levels of ARHGAP19 were assessed by immunoblotting. GAPDH was used as a loading control.

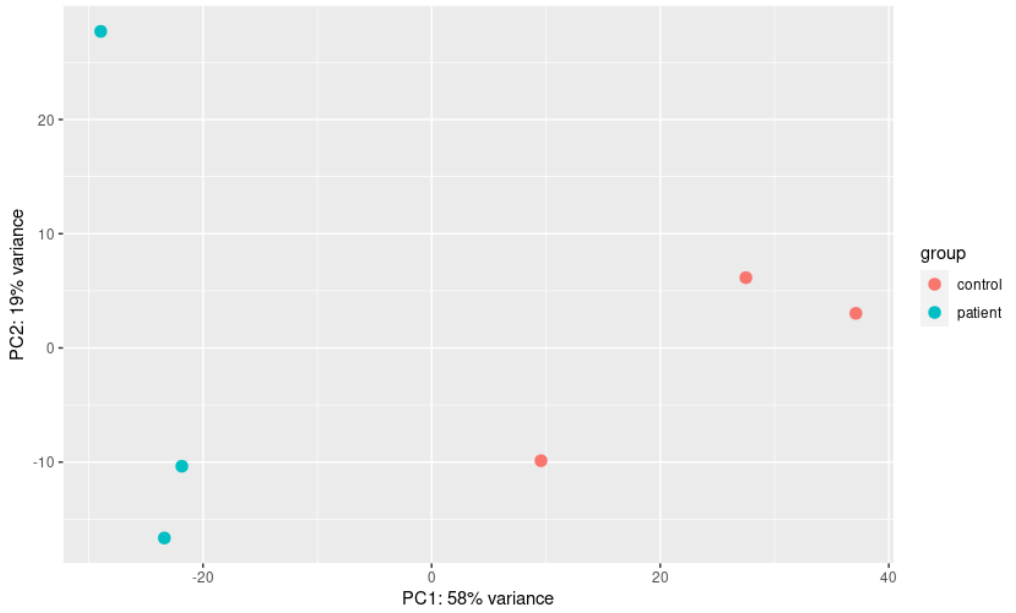

Supplemental Figure 4. RNA-Seq principal component analysis (PCA) plot. Differential expression analysis was done on 3 patients along with 3 controls, showing a separation between their RNA expression patterns.

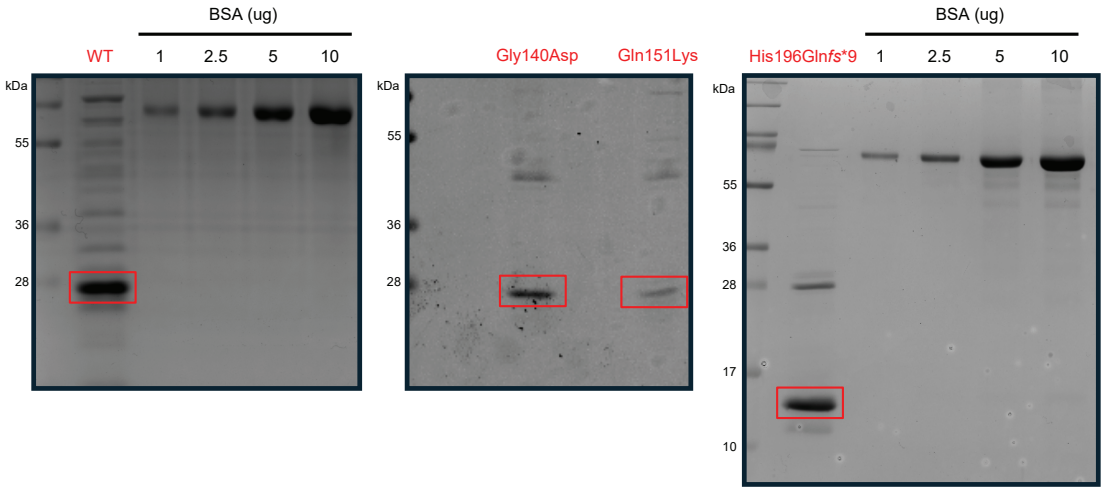

Supplemental Figure 5. Expression and purification of the ARHGAP19 GAP domains. Purified wild type (WT) ARHGAP19 GAP domain and the indicated GAP mutant proteins were resolved by SDS-PAGE with increasing amount of bovine serum albumin (BSA) standard and stained with Coomassie blue to quantify the concentration of purified ARHGAP19 GAP domains. Red boxes indicate purified ARHGAP19 GAP domains. 1.5 ug of purified ARHGAP19 wild type and mutant proteins was used for the in vitro GAP assays.

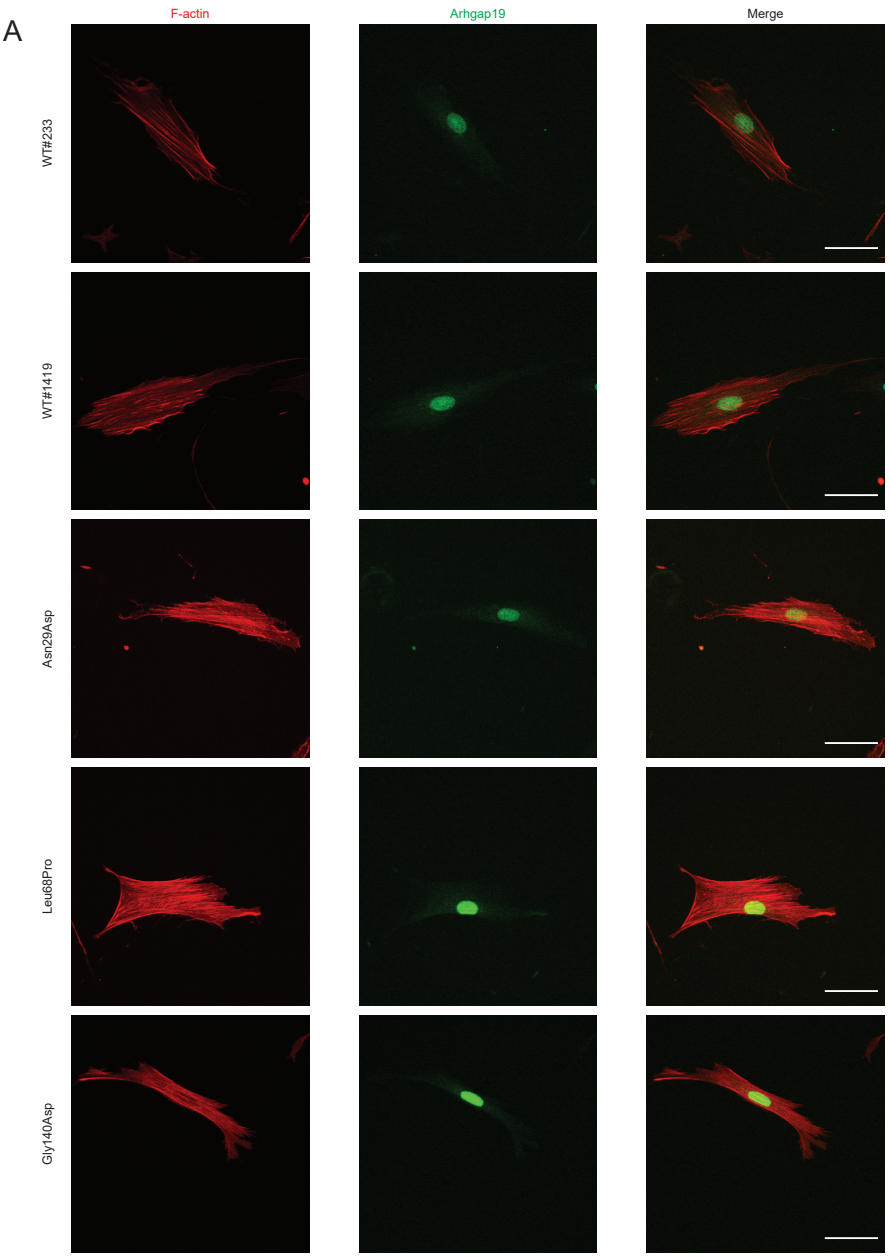
A
F-actin
Arhgap19
Merge
WT#233
WT#1419
Asn29Asp
Leu68Pro
Gly140Asp

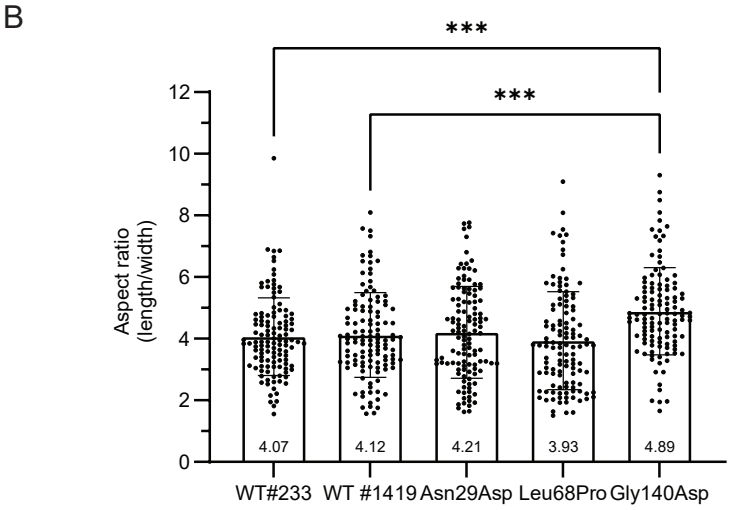
B
***
***
Aspect ratio (length/width)
0
2
4
6
8
10
12
4.07
4.12
4.21
3.93
4.89
WT#233
WT #1419
Asn29Asp
Leu68Pro
Gly140Asp

Supplemental Figure 6. Actin cytoskeleton analysis of fibroblasts from healthy controls and ARHGAP19 mutants. A. Representative images of fibroblasts from healthy controls and ARHGAP19 mutants stained with Alexa Fluor 555-conjugated phalloidin (F-actin, red) and anti-ARHGAP19 antibodies (green). Scale bar, 50 µm. B. Quantification of the aspect ratio (length/width) of fibroblasts from healthy controls and ARHGAP19 mutants. Data are presented as means ± SEM from three independent experiments of 120 cells per conditions (n=3; ***, p<0.001; one-way ANOVA).

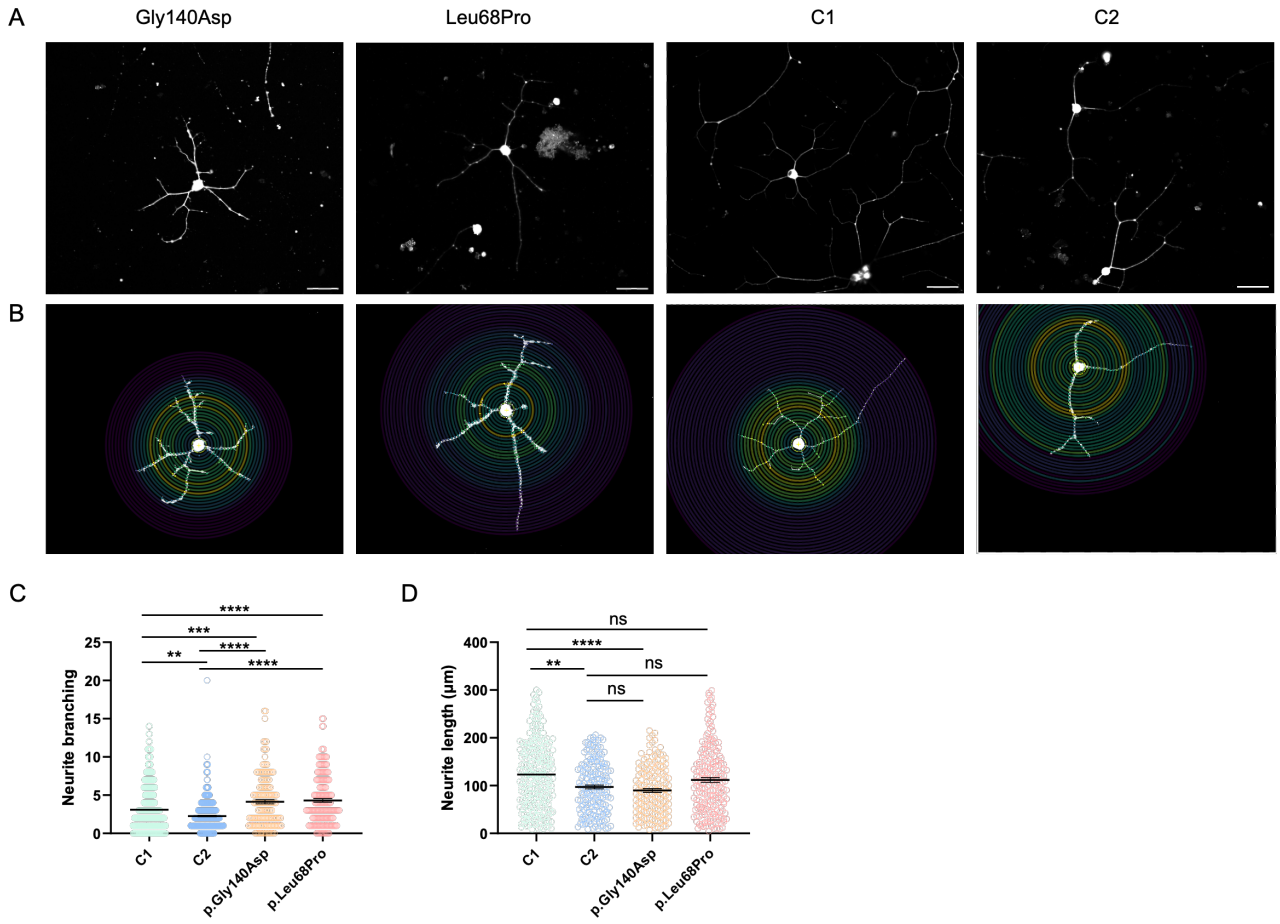

Supplemental Figure 7. Spinal motor neurons morphology and neurite branching via Sholl analysis. A. Confocal microscopy image of a spinal motor neuron of each genotype taken at 20x. Scale bar is shown at 50µm. B. Illustration of the Sholl analysis of a spinal motor neuron of each genotype (DIV18). Concentric circles spaced at 5µm intervals radiating outward from the soma are shown. C. Neurite branching and D. neurite length (µm) via Sholl analysis. Each bar represents mean (± SEM). Asterisks above the bars

indicate significant difference (*P ≤ 0.05, **P ≤ 0.01, ***P ≤ 0.001) and ns non significance. Spinal motor neuron neurites for patient derived iPSC MNs, p.Gly140Asp (orange) and p.Leu68Pro (pink) versus controls C1 (green) and C2 (blue). (n = 5-10 cells per genotype).

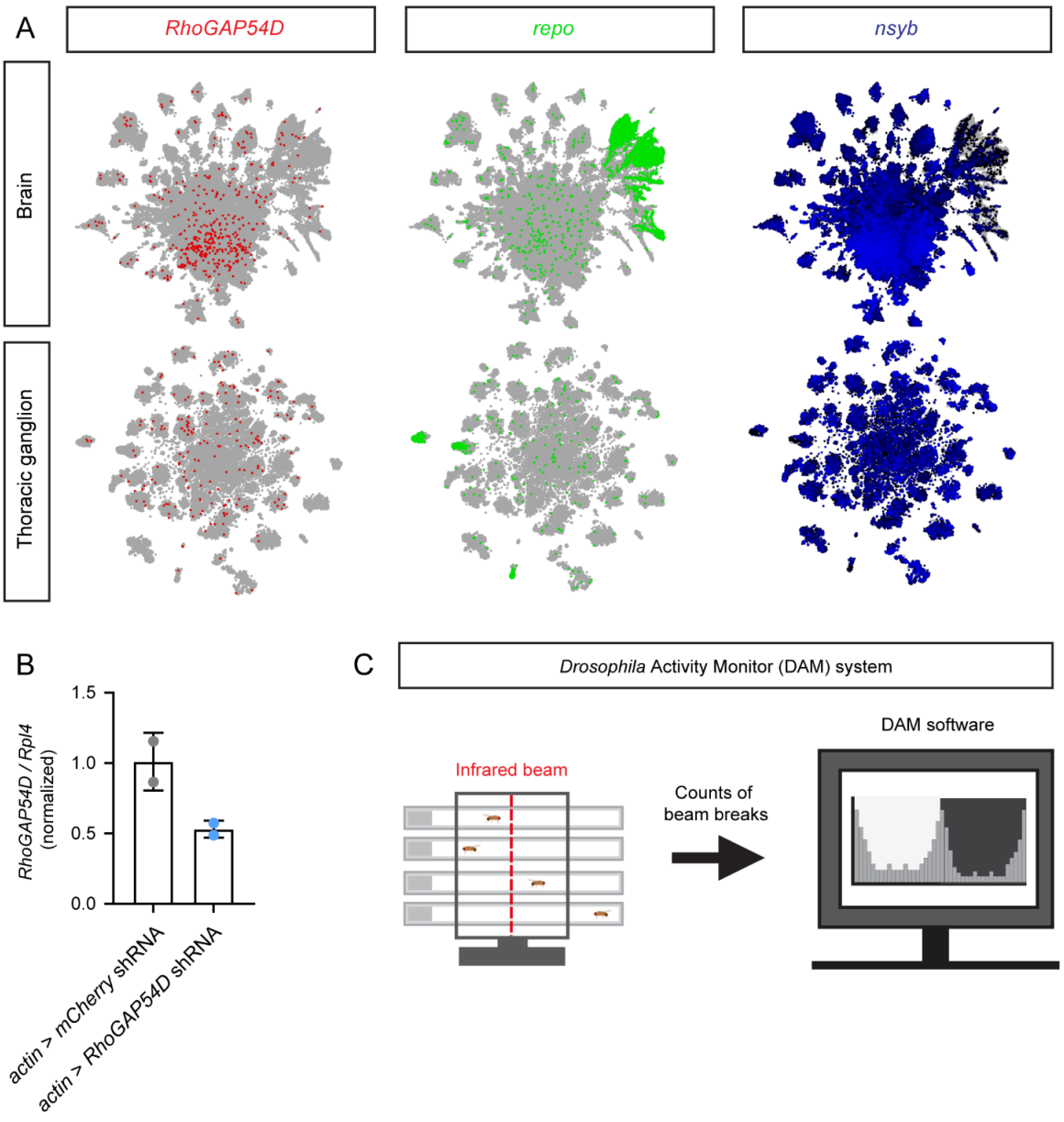

Supplemental Figure 8. A. Visualisation of single-cell RNAseq data from the adult *Drosophila* central nervous system (above) and thoracic ganglion (below) using SCOPE (13, 14). *RhoGAP54D* expression is compared to the post-mitotic glial and neuronal markers *repo* and neuronal synaptobrevin (*nsyb*). B. Validation of *RhoGAP54D* knockdown via quantitative PCR. *RhoGAP54D* expression was normalised to the *Rpl4* house-keeping gene. C. Schematic of the DAM system. Flies housed individually in glass

tubes are shown crossing a central infrared beam, allowing the number of beams breaks over time to be used as a readout of temporal changes in locomotor activity.

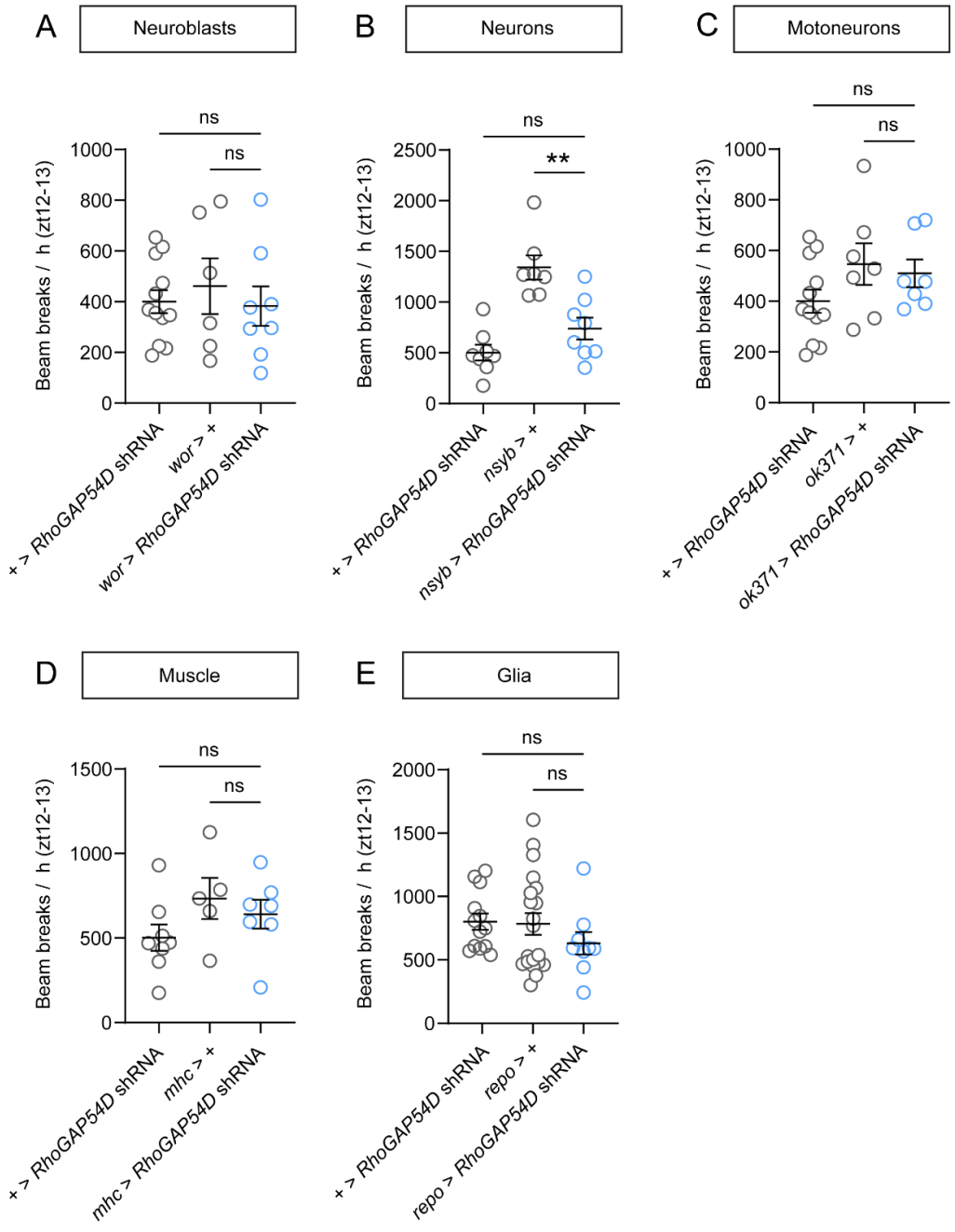

Supplemental Figure 9. A-E. Effects of *RhoGAP54D* knockdown in defined cell-types on adult *Drosophila* locomotor activity, quantified by beam breaks across 24 h in the DAM system. Specific drivers labelling neuroblasts (A, *wor*-Gal4), post-mitotic neurons (B, *nsyb*-Gal4), motoneurons (C, *ok371*-Gal4), muscle cells (D, *mhc*-Gal4), or glia (E, *repo*-Gal4), were used to drive *RhoGAP54D* shRNA. N-values are as follows for shRNA alone controls, driver alone controls, and experimental RhoGAP54D knockdown flies: A – 12, 6,

8; B – 8, 7, 8; C – 12, 7, 7; D – 8, 5, 7; E – 13, 20, 9. Central line in dot plots: mean. Error bars: SEM. **P < 0.005, ns – P < 0.05, one-way ANOVA with Dunnett's post-hoc test.

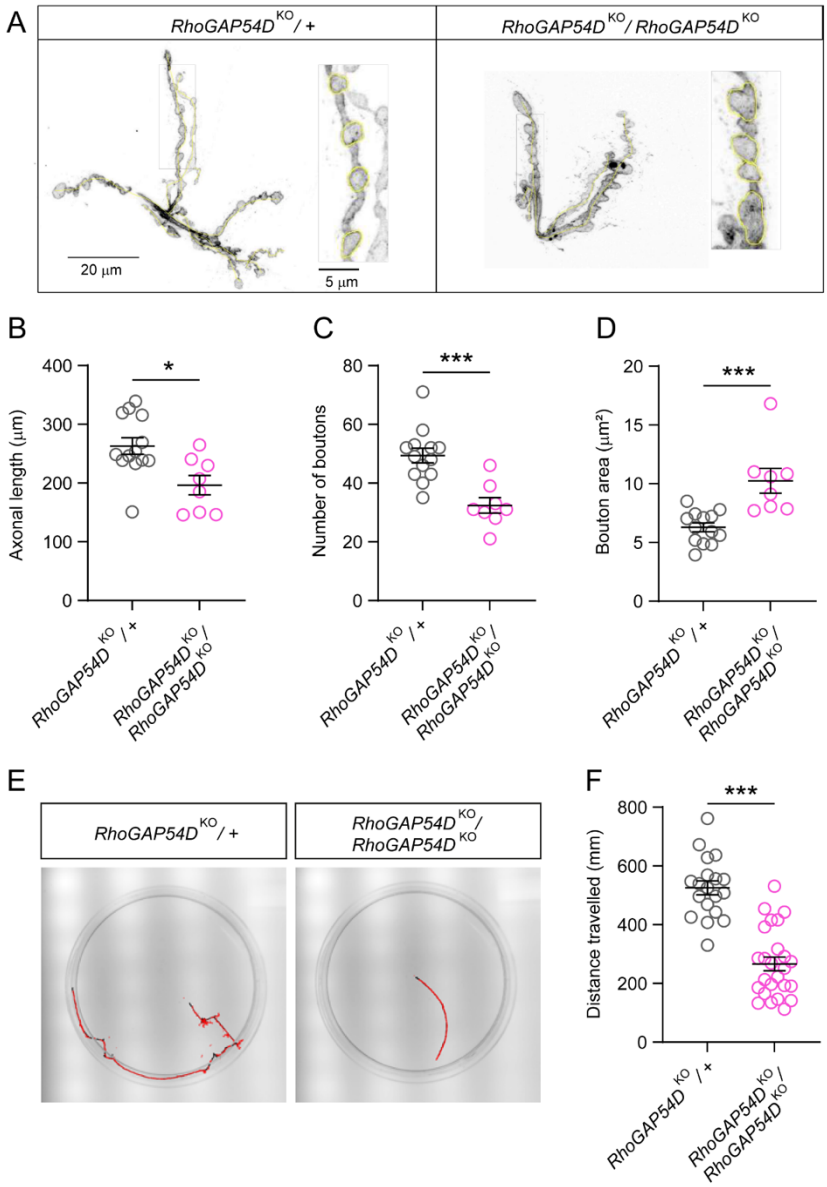

Supplemental Figure 10. A. Confocal z-stacks of representative *RhoGAP54D*^{KO} heterozygote and homozygote motoneuron axons/synapses innervating muscle 6/7, segment 3, of the 3rd instar larval body wall. Yellow lines trace axonal branches. Magnified insets show motoneuron synaptic boutons, traced in yellow. B-D. Axonal length (B), synaptic bouton number (C), and synaptic bouton area (D), in *RhoGAP54D*^{KO}

heterozygote and homozygote motoneurons. E. Traces of peristaltic locomotion in *RhoGAP54D*^{KO} heterozygote and homozygote 3rd instar larvae over 30 seconds on an agar surface. F. Mean distance travelled over 30 seconds in *RhoGAP54D*^{KO} heterozygote and homozygote larvae. *RhoGAP54D*^{KO}/+: N = 19, *RhoGAP54D*^{KO}/*RhoGAP54D*^{KO}: N = 25. Central line in dot plots: mean. Error bars: SEM. * P < 0.05, ***P < 0.0005, t-test with Welch's correction (b, d, e) or Mann-Whitney U-test (f).

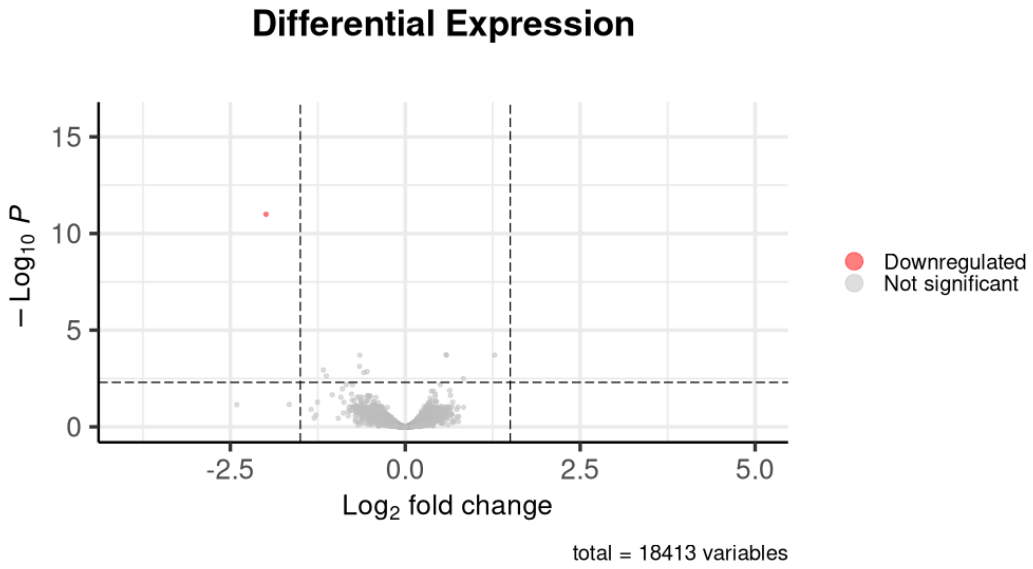

Supplemental Figure 11. RNA-Seq analysis on 48-hpf zebrafish larvae, comparing wild-type and arhgap19 CRISPants larvae. Volcano plot showed significantly up-regulated downregulated arhgap19 gene ($log_2FC = -1.99$, adjusted $P = 1.0 \times 10^{-11}$).

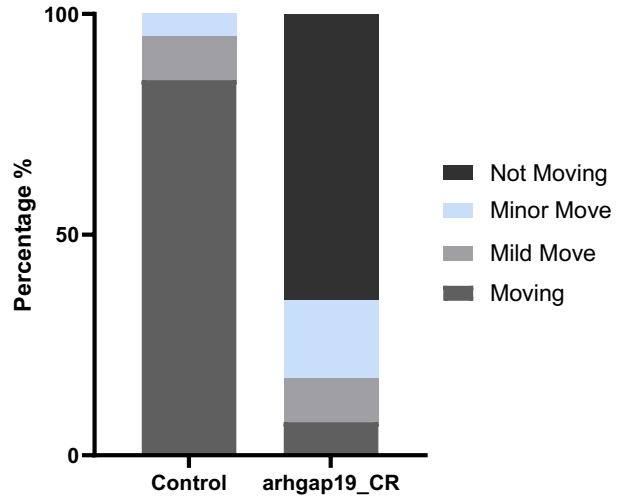

Supplemental Figure 12. Zebrafish ARHGAP19 model exhibited aberrant escape response and touch-induced swimming. Control larvae responded to touch stimulation with swimming response in 100% of 20 examined larvae, while arhgap19 Crispants significantly failed to respond to touch in 65% of 40 examined larvae, Fisher's exact test ***P<0.0001. The touch-evoked response assay was performed at 96 hpf, and scored as the percentage of examined larvae's response to touch (response: always swam away, mild: swam away multiple times, minor: swam away few times and no response: didn't swim away). Videos of these are available on request.

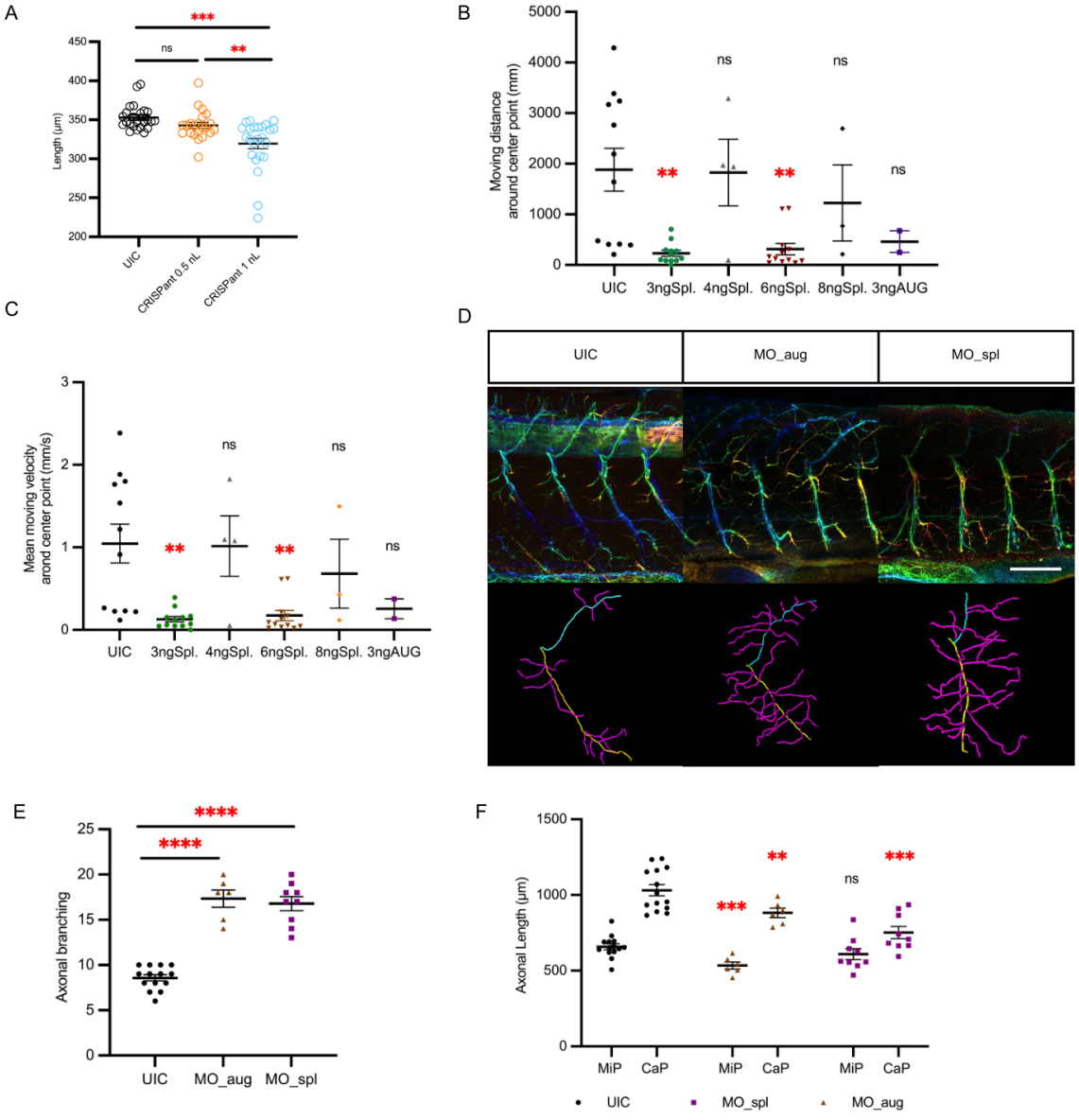

Supplemental Figure 13. A. Body length of UIC and *arhgap19* mutant zebrafish larvae at 5-dpf. B-C. Behavior analysis of UIC and morpholino-injected mutants (MOs) zebrafish

larvae at 5-dpf: Quantification of total travel distance (B) and travel velocity (C) of UIC and MOs zebrafish larvae for 30 mins (3ngSpl_MO & 6ngSpl_MO: n = 12; 4ngSpl_MO n = 4; 8ngSpl_MO n = 3; 3ngAUG_MO n = 2). Each bar represents mean (± SEM). Asterisks above the bars indicate significant difference (*P ≤ 0.05, **P ≤ 0.01, ***P ≤ 0.001, ****P ≤ 0.0001). D-F. Spinal motor neurons morphogenesis defects in MOs mutant zebrafish larvae. D. Confocal imaging analysis and three-dimensional reconstruction of spinal motor neurons in MOs mutant larvae at 5-dpf; scale bar = 100 μm. E. Axonal branching (magenta) number of Cap axons (yellow) in UIC and MOs mutant zebrafish larvae. F. Average axonal length of Cap (yellow) and Mip (blue) axons in UIC and MOs mutant zebrafish larvae. Each bar represents mean (± SEM). Asterisks above the bars indicate significant difference (*P ≤ 0.05, **P ≤ 0.01, ***P ≤ 0.001, ****P ≤ 0.0001).

Family	1	2	3	4	5	6	8	9a	9b	10	11	13	15	16	18	19
Case	PT1 (F1-II:1)	PT2 (F2-II:5)	PT3 (F3-II:1)	PT4 (F4-II:1)	PT5 (F5-II:2)	PT6 (F6-II:7)	PT8 (F8-II:2)	PT9 (F9-II:3)	PT9 (F9-II:4)	PT11 (F10-II:1)	PT12 (F11-II:2)	PT14 (F13-II:3)	PT17 (F15-II:2)	PT18 (F16-II:1)	PT20 (F18-II:1)	PT21 (F19-II:1)
Phenotype	CMT-MP	CMT2 with CS	dHMN with CS + CB	CMT2-MP	dHMN	dHMN with CS	CMT2-MP	CMT2 with CS	CMTi	CMT2-MP	CMT2-MP with CS	CMT	CMTi-MP	dHMN	HMN with CS	CMT2-MP
Age at study (years)	8	21	16	14	47	16	n/a	20	13	60	15	n/a	14**	12	10	16
Median CMAP mV	ND	9.5	12.3	8.2	4.4	8.3	0.2$^{\Delta}$	ND	ND	6.5	11.7	ND	3.7	ND	3.4	11.9
Median DML ms	ND	4.1	3.8	3.7	6.9	4.0	5.5$^{\Delta}$	ND	ND	3.6	6.6	ND	4.2	ND	3.6	2.8
Median NCV m/s	ND	46	40	56	ND	51	54$^{\Delta}$	ND	ND	56	42	ND	29	ND	33	54
Ulnar CMAP mV	ND	11.4	5.2	ND	7.6	6.0	1.7$^{\Delta}$	13.3	3.0	6.5	13.9	1.4	3.8	ND	ND	4.7
Ulnar DML ms	ND	2.7	3.2	ND	3.6	2.7	4.0$^{\Delta}$	2.5	3.0	2.7	4.3	ND	2.7	ND	ND	1.78
Ulnar NCV m/s	ND	45	40	ND	47	56	35$^{\Delta}$	49	25	58	47	39	28	ND	ND	45
Peroneal (TA) CMAP mV	3.2	ND	3.6	ND	0.2	2.5	ND	ND	ND	ND	1.3	ND	ND	ND	ND	0.37
Peroneal (TA) DML ms	4.0	ND	3	ND	5.2	5.8	ND	ND	ND	ND	6.6	ND	ND	ND	ND	3.8
Peroneal (TA) NCV m/s	30	ND	45	ND	ND	15	ND	ND	ND	ND	22	ND	ND	ND	ND	68
Peroneal (EDB) CMAP mV	Absent	Absent	Absent	Absent	Absent	ND	Absent	Absent	Absent	1.1	Absent	ND	0.7	Absent	0.87	0.04

Peroneal (EDB) DML ms	Absent	Absent	Absent	Absent	Absent	ND	Absent	Absent	Absent	5.4	Absent	ND	ND	Absent	9.24	5.2
Peroneal (EDB) NCV m/s	Absent	Absent	Absent	Absent	Absent	ND	Absent	Absent	Absent	33	Absent	ND	22	Absent	ND	ND
Tibial (AH) CMAP mV	Absent	0.02	1.7	Absent	Absent	ND	0.2	0.6	Absent	ND	Absent	ND	3.6	Absent	ND	0.38
Tibial (AH) DML ms	Absent	7.1	4.7	Absent	Absent	ND	4.1	6.6	Absent	ND	Absent	ND	6.6	Absent	ND	3.7
Tibial (AH) NCV m/s	Absent	37	19	Absent	Absent	ND	22	22	Absent	ND	Absent	ND	29	Absent	ND	ND
Median SNAP uV	ND	12	36	36	NR	44	2.7$^{\Delta}$	ND	ND	6	51	ND	16	ND	14.7	44
Median CV m/s	ND	43	43	49	NR	57	48$^{\Delta}$	ND	ND	60	ND	ND	53	ND	36.9	65
Ulnar SNAP uV	ND	20	16	ND	6.1	35	2.6$^{\Delta}$	6.7	4.3	5	24	ND	10.8	ND	ND	22
Ulnar CV m/s	ND	41	39	ND	47	52	46$^{\Delta}$	50	34	65	0	ND	37	ND	ND	54
Radial SNAP uV	ND	ND	22	ND	11.7	ND	ND	ND	ND	28	ND	ND	ND	ND	ND	30
Radial CV m/s	ND	ND	45	ND	ND	ND	ND	ND	ND	68	ND	ND	ND	ND	ND	69
Peroneal SNAP uV	ND	ND	ND	3.5	10	ND	ND	ND	ND	1	ND	ND	ND	12	16.8	Absent
Peroneal CV m/s	ND	ND	ND	36	ND	ND	ND	ND	ND	46	ND	ND	ND	ND	35.8	Absent
Sural SNAP uV	ND	Absent	11	1.8	8.7	ND	1.5	Absent	Absent	Absent	Absent	ND	Absent	14	ND	8
Sural CV m/s	ND	Absent	48	30	44	ND	30	Absent	Absent	Absent	Absent	ND	Absent	ND	ND	48

EMG	ND	Unknown	Length dep den.	ND	Length dep den.	ND	ND	ND	ND	Probably length-dependent den., some acute	Length dep den.	ND	Acute den. left ADM/FDIO on BG chronic den.	Length dep den.	Den. including paraspinal muscles	Lower limb den. with some acute changes

Supplemental Table 1. Neurophysiology data of *ARHGAP19* individuals. Left upper limb unless other very severely affected, and right lower limb (unless very severely affected) unless only one limb available. Amplitudes from most distal stimulation reported. EMG = electromyography, CMAP = compound motor action potential, CV = conduction velocity, SNAP = sensory nerve action potential, ND = not done, NA = study not available, CB = conduction block (the CB described is in bilateral tibial nerves in PT3), CS = conduction slowing, R = right, L = left, UL = upper limb, FDIO = first dorsal interosseous, ADM = abductor digiti minimi, den. = denervation, Δ right UL used * data not seen but report available only ** post IVIG study 18 months after onset.

FAMILY ID	Family 1	Family 2	Family 3	Family 4	Family 5	amily 6 & Family 1	amily 7 & Family 1	Family 8	Family 9	Family 10	Family 11	mily 12 & Family	Family 13	Family 16	Family 17	Family 18	Family 20
Number of Affected	1	1	1	1	1	2	3	1	2	1	1	2	1	1	1	1	4
TESTING/METHODOLOGY INFORMATION																	
Center Location	Brazil	UK	UK	Netherland	Spain	Turkey	UK	UK	Germany	UK	Australia	UK	UK	UK	Germany	UK	Brazil
Method of Identifying Variant	WES	WES	WES	WES	WES	WES	WGS	WES	WGS	WGS	WGS	WES/WGS	WES	WES	WES	WES	WES
Method of Validating Variant	WES	Sanger sequencing	Sanger sequencing	Sanger sequencing	Sanger sequencing	Sanger sequencing	WGS	Sanger sequencing	WGS	N/A	WGS	Sanger sequencing	Sanger sequencing	Sanger sequencing	Sanger sequencing	Sanger sequencing	WES
VARIANT DESCRIPTION																	
Genomic Position Change (GRCh38/hg38)	chr10:97265921	chr10:97263448-97263450	chr10:97235258-97235258	0:97235282-97235	0:97263614-97263	chr10:97265979	0:97263582-97263	chr10:97292627	chr10:97263554	chr10:97266097	chr10:97246333	chr10:97259559	0:97263448-97263	chr10:97263611	chr10:97259525	chr10:97263470	chr10:97259424
Genomic Position Change (GRCh37/hg19)	chr10:99025678	chr10:99023205-99023207	chr10:98995015-98995015	0:98995039-98995	0:99023371-99023	chr10:99025736	0:99023339-99023	chr10:99052384	chr10:99023311	chr10:99025854	chr10:99006090	chr10:99019316	0:99023205-99023	chr10:99023368	chr10:99019282	chr10:99023227	chr10:99019181
Coding Sequence Change (NM_001136035)	c.261dup	c.585dupA	c.1243C>T	c.1219C>T	c.419G>A	c.203T>C	c.451C>A	c.1A>G	c.479del	c.85A>G	c.932C>G	c.683T>A	c.585dupA	c.422T>G	c.717T>A	c.563del	c.818C>T
Protein Sequence Change (NP_001129507)	p.Pro88Ala*fs*43	p.His196Thr*fs**10	p.Gln415*	p.Arg407*	p.Gly140Asp	p.Leu68Pro	p.Gln151Lys	p.Met1?	p.Asn160Met*fs**21	p.Asn29Asp	p.Pro311Arg	p.Leu228His	p.His196 Th*fs**10	p.Leu141Trp	p.Asn239Lys	p.Pro188Arg*fs**5	p.Pro273Leu
Exon Number Position	2 of 12	4 of 12	9 of 12	9 of 12	4 of 12	2 of 12	4 of 12	1 of 12	4 of 12	2 of 12	7 of 12	5 of 12	4 of 12	4 of 12	Exon 5 of 12	4 of 12	5 of 12
Codon Change	C/CC	_/A	CAA/TAA	CGA/TGA	GGT/GAT	CTC/CCC	CAG/AAG	ATG/GTG	AAT/AT	AAT/GAT	CCT/CGT	CTC/CAC	_/A	TTG/TGG	AAT/AAA	CCT/CT	CCC/CTC
Consequence	Insertion	frameshift	stop gained	stop gained	missense	missense/NMD	missense	start lost	frameshift	missense	missense	missense	frameshift	missense	missense	missense	missense
Zygosity	Hom	Hom	Hom	Hom	Hom	Hom	Hom	Hom	Hom	Hom	Hom	Hom	Hom	Hom	Hom	Hom	Hom
dbSNP ID	rs767899310	rs772718801	rs757781028	rs751754099	-	rs1026767404	rs1842859321	-	-	rs754312797	-	rs562006800	rs772718801	rs755015441	-	rs760101189	rs1162465048
ALLELE FREQUENCY [Allele coun																	
gnomAD v3.1.2 (Highest subpopulation if applicable) (76,156 genomes)	0.00001315 (0.0000294 Non-Finnish European) [2/152076]	0	0.00001315 (0.00003267 South Asian) [1/251376], (0.000008795 Non-Finnish European)	0.00003287 (0.0002621 Latino/Admixed American) [4/152091], (0.0000147 Non-Finnish	0	0.000006572 (0.00002414 African/African American) [1/152165]	0	0	0	0	0	0.00002628 (0.001 South Asian) [4/152192]	0	0	0	0.000006576 (0.0002076 South Asian) [1/152065]	0
gnomAD v2.1.1 (Highest subpopulation if applicable) (15,708 genomes and 125,748 exomes)	0.00003181 (0.00006154 Non-Finnish European) [7/251464]	0.00002784 (0.0001848 Finnish) [4/251439], (0.00002638 Non-Finnish European) [3/251439]	0.00001591 (0.0004139 South Asian) [2/152140]	0.00003978 (0.0000868 Latino) [3/251344], (0.00006533 South Asian) [5/251344], (0.00004399 Non-Finnish European)	0	0.000003976 (0.00002891 Latino) [1/251491]	0	0	0	0	0	0.00009543 (0.001 South Asian) [24/251464]	0.00002784 (0.0001848 Finnish) [4/251439], (0.00002638 Non-Finnish European) [3/251439]	0.000003979 (0.00003267 South Asian) [1/251345]	0	0.00005568 (0.0004573 South Asian) [14/251438]	0
Ensembl (Highest frequency observed)	< 0.01	< 0.01	< 0.01	< 0.01	N/A	< 0.01	< 0.01	N/A	N/A	< 0.01	N/A	< 0.01	< 0.01	< 0.01	N/A	< 0.01	< 0.01
Iranome (~800 exomes)	0	0	0	0	0	0	0	0	0	0	0	0	0	0	0	0	0
GME Variome (~2,500 exomes)	0	0	0	0	0	0	0	0	0	0	0	0	0	0	0	0	0
UK Biobank (394,841 exomes)	0	0	0.00000271782	0	0	0	0	0.0000298948	0	0.00002174138	0	0	0	0	0	0	0.0000013589
TOPMed (132,345 genomes)	0.000023891	0.000007964	0	0.000015928	0	0.000015928	0	0	0	0	0	0	0.000007964	0	0	0.000007964	0.000007964
54KJPN (~54,000 genomes)	0	0	0	0	0	0	0	0	0	0	0	0	0	0	0	0	0
QSG Database (23741 exomes)	0	0	1 hom	0	0	0	0	0	0	0	0	2 hom	0	0	0	0	0
CO PREDICTIONS AND CLASSIFIC																	
GERP	3.11	2.64	1.57	-1.56	5.87	2.63	3.94	2	-	2.63	5.66	2.46	2.64	3.94	2.97	3.94	5.11
CADD_Phred	-	34	39	35	26.3	28	26.2	22.6		23.7	27.5	27.6	34	29.2	-	27	27.1
Polyphen-2	-	-	-	-	PD 1	PD 0.987	PD 0.996	B 0	-	PD 0.57	PD 1	PD 0.998	-	PD 1	-	PD 0.998	-
SIFT	-	-	-	-	D 0	D 0.01	D 0	D 0	-	D 0.21	D 0	D 0	-	D 0	0.004	D 0	0.003
PROVEAN	-	D-14.45	N -1.66	N -2.25	D -6.72	D -2.75	D -3.58	N -0.68	N -1.15	N -0.28	D -7.95	D -6.07	D -14.45	D -5.33	D -4.93	-	D -9.23
MutationTaster	-	DC 1 NMD	DC 0.99 NMD	DC 0.99 NMD	DC 0.99	DC 0.99	DC 0.99	DC 1	DC 1 NMD	DC 0.503	DC 0.99	DC 0.99	DC 1 NMD	DC 0.99	DC 0.99	DC 0.99	DC 1
ACMG Clinical Significance Classification	Pathogenic (PVS1, PM2, PM4, PP1, PP3)	Pathogenic (PS3, PM1, PM2, PM4, PP1, PP3)	Pathogenic (PVS1, PM2, PM4, PP1, PP3)	Pathogenic (PVS1, PM2, PP3)	Pathogenic (PS3, PM1, PM2, PP1, PP3)	Likely Pathogenic (PS4, PM2, PP1, PP3)	Pathogenic (PS3, PS4, PM1, PM2, PP1, PP3)	VUS (PM2, PP1, PP3)	Pathogenic (PM1, PM2, PM4, PP1, PP3)	Likely Pathogenic (PS3, PM2, PP3)	Likely Pathogenic (PS4, PM2, PP1, PP3)	Pathogenic (PS4, PM1, PM2, PP1, PP3)	Likely Pathogenic (PS3, PM1, PM2, PP3)	Likely Pathogenic (PM1, PM2, PP1, PP3)	Likely Pathogenic (PM1, PM2, PP1, PP3)	Pathogenic (PM1, PM2, PM4, PP1, PP3)	VUS (PM1, PM2, PP3)

Supplemental Table 2. *ARHGAP19* variants table. Abbreviations: ACMG - American College of Medical Genetics and Genomics, CADD - Combined Annotation Dependent Depletion, Comp Het - Compound Heterozygous, D – Damaging, DC - Disease causing, Del – Deleterious, GERP - Genomic Evolutionary Rate Profiling, GME - The Greater Middle East, Hom – Homozygous, N – Natural, N/A - Not available, Not applicable, PD - Probably Damaging, PM/_M- Pathogenic Moderate, PP/_P - Pathogenic Supporting, PS/_S - Pathogenic Strong, PSD - Possibly Damaging, PVS/_VS - Pathogenic Very Strong, QSG - Queen Square Genomics, RoH - Region of Homozygosity, SNP - Single Nucleotide Polymorphism, Tol – Tolerated, WES - Whole Exome Sequencing.

Sequence	Animal species	Uniprot accession code
HUMAN ARHGAP19	*Homo sapiens*	Q14CB8
CHINPANZEE ARHGAP19	*Pan troglodytes*	K7DQC3
MACAQUE ARHGAP19	*Macaca mulatta*	H9G104
MOUSE Arhgap19	*Mus musculus*	Q8BRH3
RAT Arhgap19	*Rattus norvegicus*	M0R5V4
BOVINE ARHGAP19	*Bos taurus*	F1MGB9
DOG ARHGAP19	*Canis lupus familiaris*	F6UNS4
CHICKEN ARHGAP19	*Gallus gallus*	Q5F3G0
FROG arhgap19	*Xenopus laevis*	Q6INE5
ZEBRAFISH arhgap19	*Danio rerio*	F6NW06
FRUIT FLY RhoGAP54D	*Drosophila melanogaster*	Q8IGY7

Supplemental Table 3. UniProt accession codes used for Multiple Sequence Alignment of ARHGAP19 orthologs.

Variant (c.)	AA change (p.)	AlphaMissense pathogenicity**	AlphaMissense Class
c.85A>G	p. Asn29Asp	0.0882	likely_benign
c.203T>C	p.Leu68Pro	0.9953	likely_pathogenic
c.419G>A	p.Gly140Asp	0.9985	likely_pathogenic
c.422T>G	p.Leu141Trp	0.9915	likely_pathogenic
c.451C>A	p.Gln151Lys	0.7953	likely_pathogenic
c.683T>A	p.Leu228His	0.8643	likely_pathogenic
c.717T>A	p.Asn239Lys	0.9058	likely_pathogenic
c.818C>T	p.Pro273Leu	0.9793	likely_pathogenic
c.932C>G	p.Pro311Arg	0.9945	likely_pathogenic

Supplemental Table 4. Extracted AlphaMissense scores and associated predicted variant impact for identified *ARHGAP19* missense variants (in yellow shade are variants located within the GAP domain).

crRNA	Forward primer	Reverse primer
1	ACACTCTTTCCCTACACGACGCTCTTCCGATCTggttgctgtttcccctactat	GACTGGAGTTCAGACGTGTGCTCTTCCGATCTagtgtggatgatgaacCTGTGA
2	ACACTCTTTCCCTACACGACGCTCTTCCGATCTccggaaatatgttaggaccattg	GACTGGAGTTCAGACGTGTGCTCTTCCGATCTAGGTCACTGGCATTCATctga
3	ACACTCTTTCCCTACACGACGCTCTTCCGATCTggttgctgtttcccctactat	GACTGGAGTTCAGACGTGTGCTCTTCCGATCTgtgtggatgatgaacCTGTGA
4	ACACTCTTTCCCTACACGACGCTCTTCCGATCTGGCCGCCCATTATCTTCAAC	GACTGGAGTTCAGACGTGTGCTCTTCCGATCTgtctgcaattttggacgca
5	ACACTCTTTCCCTACACGACGCTCTTCCGATCTaattgtgggttgctgtttcc	GACTGGAGTTCAGACGTGTGCTCTTCCGATCTcagctaatgatgtagaaggcaca
6	ACACTCTTTCCCTACACGACGCTCTTCCGATCTtgtttacaccctgacacagtt	GACTGGAGTTCAGACGTGTGCTCTTCCGATCTTGTTTGGCGGTGTGGTAGA

Supplemental Table 5. Primers for NGS sequencing (MiSeq).

Primer name	Primer sequence
ARHGAP19 qPCR forward	GGCATCAAAGGATGACCTTG
ARHGAP19 qPCR reverse	CTTTGCTGACTCTGGCATATC
RPL18A qPCR forward	CCCACAACATGTACCGGGAA
RPL18A qPCR reverse	TCTTGGAGTCGTGGAACTGC

Supplemental Table 6. qPCR primers

Stock name	Genotype	Source
actin-Gal4	*y[1] w[*]; P{Act5C-GAL4-w}E1/CyO*	BDSC #25374
UAS-RhoGAP54D shRNA	[1] *v[1]; P{y[+t7.7] v[+t1.8]=TRiP.HMS03522}attP40*	BDSC #54051
RhoGAP54D-Gal4	y[1] w[*]; TI{GFP[3xP3.cLa]=CRIMIC.TG4.1}RhoGAP54D[CR02433-TG4.1]/SM6a	BDSC #92267
deGradFP	w[*]; P{w[+mC]=UAS-Nslmb-vhhGFP4}3	BDSC #38421
GFP:RhoGAP54D	w*; GFP:RhoGAP54D / CyO	(16)
	yw; UAS-CD4::TdTom	unknown
	UAS-mCherry shRNA	unknown
RhoGAP54D null allele	w*; RhoGAP54D^{KO} / CyO	Gift from Bellaïche lab
Tubulin-Gal4	Tub-Gal4 / Tm6b	Gift from Southall lab
	w*; GFP:RhoGAP54D / CyO ; Tub-Gal4 / Tm6b	This study
	w*; GFP:RhoGAP54D / CyO ; UAS-Nslmb-vhhGFP4 / TM6b	This study

Supplemental Table 7. Drosophila stocks.

Genotype	Source
w[*]; P{w[+mC]=wor.GAL4.A}2	Kind gift from Dr. Tony Southall, Imperial College London, UK
w[1118]; P{w[+mW.hs]=GawB}VGlut1[OK371]	Gift from Prof. Kyunghee Koh, Thomas Jefferson University, USA
w[*]; P{w[+mC]=Mhc-GAL4.K}2/TM3, Sb[1]	BDSC #55133
y[1] w[1118]; P{y[+t7.7] w[+mC]=nSyb-GAL4.P}attP2	BDSC #51941
P{w[+mC]=repo-Gal4.L}Oatp30B[repoF3]	Kind gift from Dr. Vilaiwan Fernandes, University College London, UK

Supplemental Table 8. Tissue specific drivers for Gal4 expression of RhoGAP54D shRNA.

Variant	Predicted variant impact (AlphaMissense)	ARHGAP19 protein level in patient fibroblasts	ARHGAP19 protein level in patient iPSC MNs	GAP activity	Healing assay (patient fibroblasts)	Migration assay (patient fibroblasts)
c.1A>G , p.Met1?	n/a			*		
c.85A>G, p.Asn29Asp	Likely benign	No change	Reduced	*	Defective	Defective
c.203T>C, p.Leu68Pro	Likely pathogenic	No change	Reduced	*	Non-defective	Non-defective
c.261dup, p.Pro88Ala*fs**43	n/a			*		
c.419G>A, p.Gly140Asp	Likely pathogenic	No change	Reduced	Defective	Defective	Defective
c.422T>G, p.Leu141Trp	Likely pathogenic			n/a		
c.451C>A, p.Gln151Lys	Likely pathogenic			Defective		
c.479del, p.Asn160Met*fs**21	n/a			n/a		
c.563del, p.Pro188Arg*fs**5	n/a			n/a		
c.585dupA , p.His196 Thr*fs**10	n/a			Defective		
c.683T>A, p.Leu228His	Likely pathogenic			n/a		
c.717T>A, p.Asn239Lys	Likely pathogenic			n/a		
c.818C>T, p.Pro273Leu	Likely pathogenic			n/a		
c.932C>G, p.Pro311Arg	Likely pathogenic			*		
c.1219C>T, p.Arg407*	n/a			*		
c.1243C>T, p.Gln415*	n/a			*		

Supplemental Table 9. Molecular effect of ARHGAP19 variants. Variants within the functional GAP domain are shaded in grey. n/a: not tested. MNs: motor neurons. *: GAP activity assay cannot be performed on variants outside the GAP domain. Where effect is blank denotes patient material was unavailable.